*Quantum Electronics* **48** (3) 215–221 (2018) ©2018 Kvantovaya Elektronika and Turpion Ltd

https://doi.org/10.1070/QEL16529

# Amplified luminescence of heavily doped $Al_xGa_{1-x}N$ structures under optical pumping

P.A. Bokhan, K.S. Zhuravlev, D.E. Zakrevskii, T.V. Malin, I.V. Osinnykh, N.V. Fateev

***Abstract.*** **Spectral, temporal, and polarisation characteristics of luminescence of heavily doped $Al_xGa_{1-x}N$ films on a sapphire substrate are studied under pulsed pumping at the wavelength $\lambda$ = 266 m. Spectra of spontaneous emission related to donor–acceptor transitions are inhomogeneously broadened with the FWHM of above 0.5 eV and cover the entire visible range. Spectra of radiation emitted from an edge of investigated structure comprise several narrow-band equidistant components, each of them being split to TE and TM modes with mutually orthogonal polarisations. This is related to plane waves propagating inside a plane waveguide along a zigzag path in the conditions of total internal reflection from waveguide surfaces. The optical gains measured for $Al_{0.5}Ga_{0.5}N/AlN$ at $\lambda \approx$ 510 nm, $Al_{0.74}Ga_{0.26}N/AlN$ at $\lambda \approx$ 468 nm, and $AlN/Al_{0.6}Ga_{0.4}N/AlN/Al_2O_3$ at $\lambda \approx$ 480 nm were, respectively, ~70, 20, and 44 $cm^{-1}$. The luminescence quantum efficiencies measured for $Al_{0.74}Ga_{0.26}N$, $Al_{0.65}Ga_{0.35}N$, and $Al_{0.5}Ga_{0.5}N$ films are, respectively, 0.79, 0.49, and 0.14; the transition cross sections calculated at emission band centres are ~$10^{-18}$ $cm^2$.**

***Keywords:*** *luminescence, optical pumping, spontaneous emission, gain.*

## 1. Introduction

Semiconductor laser sources due to a wide wavelength radiation range, compactness, high-efficiency, reliability, low cost, and simple employment are used in many fields of science and technology. In recent years, much attention has been paid to studying and producing light emitting media based on $Al_xGa_{1-x}N$ structures, which are characterised by the width of forbidden bandgap varied from 3.4 eV (for GaN) to 6.1 eV (for AlN) with direct optical transitions between conduction and valence bands [1–3]. It makes these structures promising for producing light devices emitting in a wide spectral band ranging from UV to near-IR [4–11]. Visible light emitting diodes and lasers, especially with true green emission corresponding to the maximal sensitivity of mesopic vision in 500–550 nm and 'white' wideband emission in a single emitting element, are required in many applications. These are fast telecommunication; laser ground-based (submarine) location devices and rangefinders; systems for aircraft landing and ship steering; devices for illumination, target designation, topographic tracking, high-speed interferometry and photography; information indication and display including television; projection devices, optical coherent tomographs, photodynamic therapy; spectral radiation sources; master oscillators and pump sources for dye lasers, solid-state lasers, fibre lasers including those used for isotope separation; energy-saving and ecological general-purpose light sources with a continuous spectrum and high light and energy efficiency, and so on.

Luminescence of $Al_xGa_{1-x}N$ structures with various aluminium mole contents $x$ grown by the molecular epitaxy method on sapphire substrates was studied in [12] under excitation by a low-energy (below 20 keV) electron beam of up to 200 kW power. In cathode luminescence spectra of $Al_xGa_{1-x}N$ structures at $x > 0.42$ heavily doped with silica, a wideband emission was observed that covered the visible and near-IR spectral ranges at $\lambda$ = 460–720 nm (corresponding to quantum energies of 1.72–2.7 eV), the side luminescence being negligible. Later it was shown [13] that this luminescence is related to transitions through levels of emitting centres comprising a doped atom and a point defect of crystal lattice, i.e., to donor-acceptor transitions with acceptor participation. When $Al_xGa_{1-x}N$ layers were excited by a linear electron beam, the emission detected at sample edges had a mode structure and exhibited superradiance properties. This makes us assume that coherent and incoherent light sources can be produced on the basis of $Al_xGa_{1-x}N$ structures, capable of operating at various wavelengths, including sources tunable in a wide spectral range.

The present work is aimed at studying spectral, temporal, and polarisation characteristics of spontaneous and amplified luminescence in $Al_xGa_{1-x}N$ structures under optical pumping and at measuring the quantum efficiency and optical gain in structures in question.

## 2. Experimental setup and main results

The structures to be studied were grown by the molecular epitaxy method in a modified Riber CBF-32 installation. The technology of synthesis and the process of film parameter

**P.A. Bokhan, T.V. Malin** A.V. Rzhanov Institute of Semiconductor Physics, Siberian Branch, Russian Academy of Sciences, prosp. Akad. Lavrent'eva 13, 630090 Novosibirsk, Russia; e-mail: bokhan@isp.nsc.ru, zhur@ isp.nsc.ru, mal-tv@isp.nsc.ru, osinus-sb@ isp.nsc.ru;
**D.E. Zakrevskii** A.V. Rzhanov Institute of Semiconductor Physics, Siberian Branch, Russian Academy of Sciences, prosp. Akad. Lavrent'eva 13, 630090 Novosibirsk, Russia; Novosibirsk State Technical University, prosp. Karla Marksa 20, 630092 Novosibirsk, Russia; e-mail: zakrdm@isp.nsc.ru;
**K.S. Zhuravlev, I.V. Osinnykh, N.V. Fateev** A.V. Rzhanov Institute of Semiconductor Physics, Siberian Branch, Russian Academy of Sciences, prosp. Akad. Lavrent'eva 13, 630090 Novosibirsk, Russia; Novosibirsk State University, ul. Pirogova 2, 630090 Novosibirsk, Russia; e-mail: fateev@isp.nsc.ru

Received 9 October 2017; revision received 29 December 2017
*Kvantovaya Elektronika* **48** (3) 215–221 (2018)
Translated by N.A. Raspopov

measurements are thoroughly described in [13, 14]. The source of active nitrogen was an ammonia flow (130 $cm^3$ $min^{-1}$), and the source of impurity (doping) silica atoms was a mixture of silane (~0.7%) and nitrogen at a constant gas mixture flow velocity of ~3 $cm^3$ $min^{-1}$. In preliminary experiments it was established that in this dopant flow, the intensities of cathode- and photoluminescence were maximal in $Al_{0.62}Ga_{0.38}N$ films. In $Al_xGa_{1-x}N$ films with greater $x$, the silica concentration $n_{Si}$ was (3 – 1) × $10^{20}$ $cm^{-3}$, and concentration of free electrons $n_e$ was (24–0.1) × $10^{18}$ $cm^{-3}$ [15].

Structures with an $Al_xGa_{1-x}N$ active layer and AlN buffer layer on sapphire $AlGaN/AlN/Al_2O_3$ were studied. $Al_xGa_{1-x}N$ films of various compositions ($x$ = 0.42–1) with a thickness $h_0$ = 1.2 μm were grown on azotised sapphire substrates having a (0001) orientation and thickness $h$ = 430 μm with an AlN buffer layer of thickness $h_p$ = 320 nm. In addition, an $AlN/Al_{0.6}Ga_{0.4}N/AlN/Al_2O_3$ structures with the layer thicknesses $h_{p1}$ = 25 nm, $h_0$ = 600 nm, $h_{p2}$ = 250 nm and a substrate thickness $h$ = 430 nm were investigated. All the samples had the size of 15 × 10 mm and were produced by cleaving the structure along sapphire crystallographic planes. Luminescence properties were studied under optical pumping, which presents more possibilities than electron-beam pumping. The samples were pumped from the side of the AlGaN film by the forth harmonic of a pulsed Nd:YAG laser at $\lambda$ = 266 nm with the pulse FWHM duration of 8 ns at a pulse repetition rate of 10 Hz. The pump radiation was directed normally to a sample surface and had the shape of a 0.04-cm-wide uniform strip with a regulated length of the excitation zone $L$ = 0–1 cm varied in steps of 10 μm. The maximal density of the pump pulse power $P_p$ on the sample surface reached ~9 MW $cm^{-2}$ at the intensity nonuniformity along the strip length of less than 5%.

All experiments were carried out at room temperature. Spontaneous emission (SE) parameters were measured at an angle of 45° to the sample surface (Fig. 1a). Simultaneously, the emission passing from a structure edge was detected (Fig. 1b), which, as will be shown below, is an amplified spontaneous emission (ASE) by nature. The spectra were recorded in the range 200–750 nm by a spectrometer with a high dynamic range and the spectral resolution of ~0.5 nm [16]. Time evolution of the luminescence intensity was measured by using a prism monochromator and a FEU-106 photomultiplier. An electric signal from the latter was detected and averaged over 100 laser pulses by a Tektronix 2024 oscilloscope with a time resolution of 3 ns. The radiation passed to spectrometers through a multimode silica fibre and for comparative measurements it was focused directly onto the entry slit of the spectrometer. In both cases, the photoluminescence spectra recorded were identical. Optical gains in studied samples were measured by the single-pass method [17, 18]. Amplification arising in the samples was identified by an exponential growth of the output emission intensity in longer excitation zones and by narrow peaks formed in the spectra.

Luminescence quantum yields in $Al_xGa_{1-x}N$ films were measured relative to the luminescence quantum yields of the R6G dye solution in ethanol, which served as a reference with the known quantum yield of 0.95 [19]. The dye inside a thin (a thickness of 2 mm) quartz cell and the samples were excited (in the same pumping and recording geometry) by the radiation beam with a diameter of 8 mm at $\lambda$ = 266 nm having a uniform intensity distribution, which passed to a sample surface at an angle of 45°. The intensity of spontaneous emission

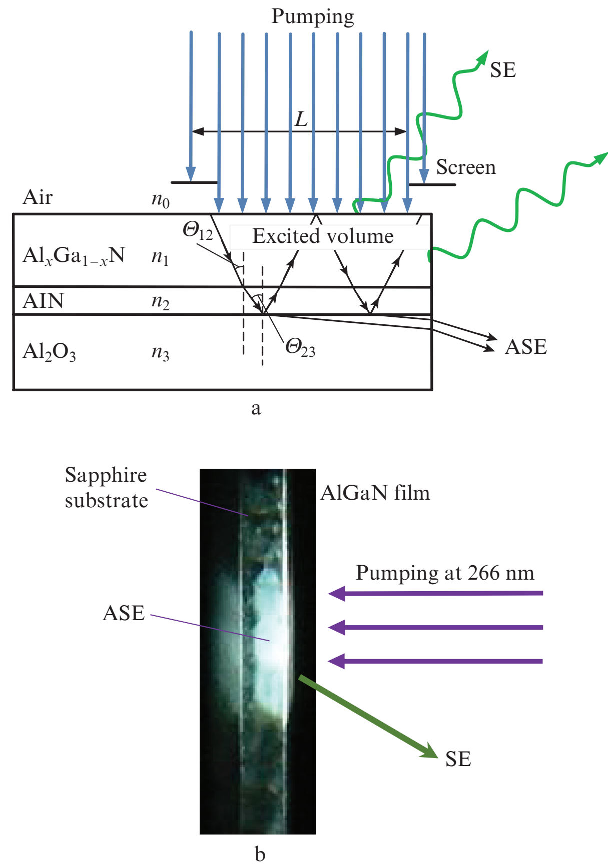


**Figure 1.** (a) Schematic of luminescence excitation and detection in $Al_xGa_{1-x}N/AlN/Al_2O_3$ structures and (b) photographs of a cleaved edge in an $Al_{0.65}Ga_{0.35}N/AlN/Al_2O_3$ structure at the instant of pumping by a laser pulse at $\lambda$ = 266 nm.

was measured by a wide-aperture (the diameter of 9.5 mm) calibrated photodetector placed at a distance of 15 mm from the sample surface in the normal direction.

Figures 2 and 3 present typical SE (Fig. 2a) and ASE (Fig. 2b) spectra for $Al_xGa_{1-x}N/AlN/Al_2O_3$ with $x$ = 0.74, 0.6, and 0.5 and for $AlN/Al_{0.6}Ga_{0.4}N/AlN/Al_2O_3$ (Fig. 3). Similarly to the pumping by an electron beam (see [12]), spectra of all structures with $x$ > 0.4 comprise a single wide band and side bands are absent. The emission spectrum is in the visible range and has a FWHM width $\Delta\lambda_{1/2}$ ≈ 150 nm. This is above the similar values for IR emission of superluminescent diodes on heterostructures with quantum-well active layers [20–23] and of a Ti:sapphire laser [24, 25]. At a higher aluminium content, the emission bands shift to the UV-range, with the spectrum FWHM width slightly varying. In the frequency region the width varies inversely proportional to the wavelength and reaches 400 THz.

The spectra detected from a cleaved edge of the structure (ASE spectra) are split to almost equidistant peaks. For example, in the $Al_{0.5}Ga_{0.5}N$ structure the band maxima are observed at the wavelengths $\lambda$ ≈ 435, 477, 528, 595, and 680 nm with the interval of ~2100 $cm^{-1}$ between them.

ASE spectra for $Al_{0.5}Ga_{0.5}N$ are shown in Fig. 4 at the pump power density $P_p$ ≈ 0.006, 0.2, 4, 40, 100, and 1000 kW $cm^{-2}$ and excitation zone length $L$ = 1.2 mm.

Figure 5 demonstrates the dependences of SE and ASE intensities for the $Al_{0.5}Ga_{0.5}N$ film on the pump power density

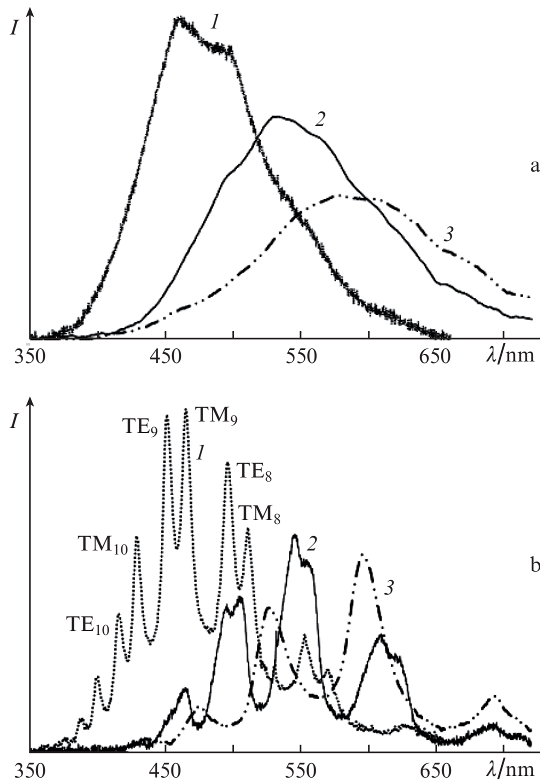


**Figure 2.** Luminescence spectra of (a) SE and (b) ASE in (*1*) $Al_{0.74}Ga_{0.26}N/AlN$, (*2*) $Al_{0.6}Ga_{0.4}N/AlN$, and (*3*) $Al_{0.5}Ga_{0.5}N/AlN$ structures at the pump power density $P_p$ = 300 kW cm$^{-2}$.

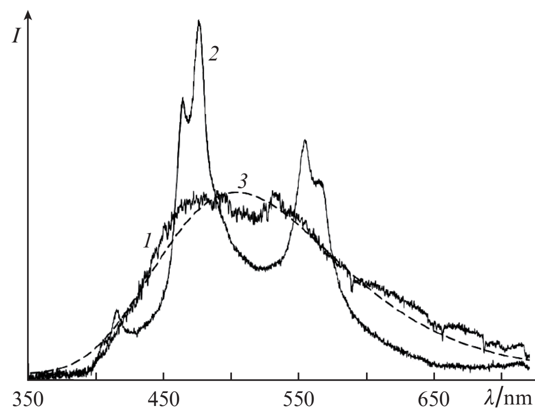


**Figure 3.** Luminescence spectra of (*1*) SE and (*2*) ASE in the $Al_{0.6}Ga_{0.4}N/AlN/Al_2O_3$ structure at the pump power density $P_p$ = 300 kW cm$^{-2}$; (*3*) Gaussian approximation.

at $L$ = 0.6 and 1.2 mm. The ASE intensity sharply increases in the range $P_p \approx 15-25$ kW cm$^{-2}$, and grows almost linearly with the pump power above $P_p \approx 60$ kW cm$^{-2}$. On the contrary, the SE intensity is almost linear in the whole range of $P_p$ variation.

In Fig. 6 one can see fragments of ASE spectra for the $Al_{0.5}Ga_{0.5}N$ film measured without a polariser and with it at various turn angles of the latter $\zeta$. Two groups of ASE bands are observed with different positions of maxima.

Dependences of the ASE intensity $I$ for various structures on the length of excitation zone $L$ are shown in Fig. 7. One

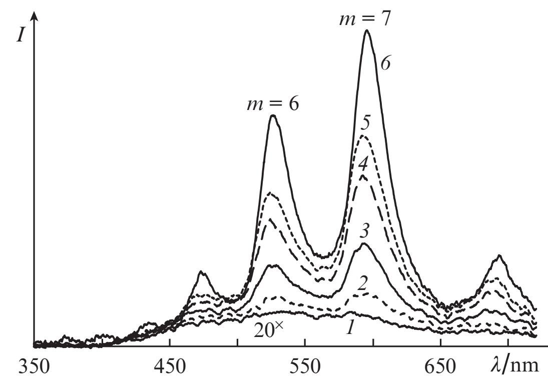


**Figure 4.** Luminescence spectra of ASE in the $Al_{0.5}Ga_{0.5}N$ structure at the pump power density $P_p$ = (*1*) 0.006, (*2*) 0.2, (*3*) 4, (*4*) 40, (*5*) 100, and (*6*) 1000 kW cm$^{-2}$ ($m$ is the mode order).

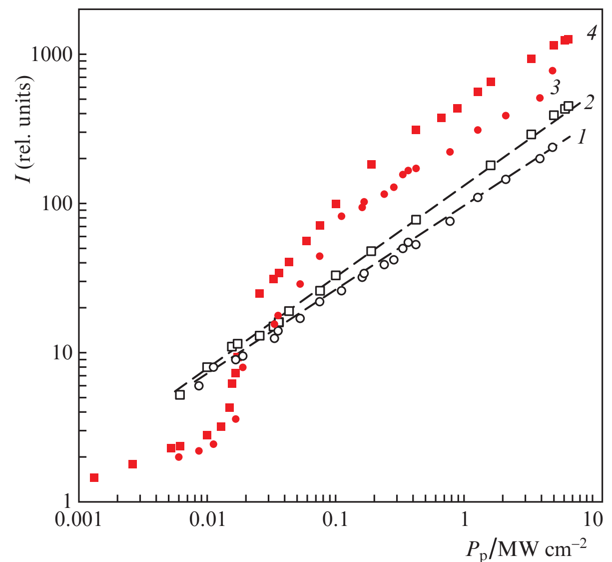


**Figure 5.** Intensity of (*1*, *2*) SE and (*3*, *4*) ASE luminescence in the $Al_{0.5}Ga_{0.5}N$ structure at $\lambda$ = (*1*, *2*) 560 and (*3*, *4*) 528 nm and $L$ = (*1*, *3*) 0.6 and (*2*, *4*) 1.2 mm.

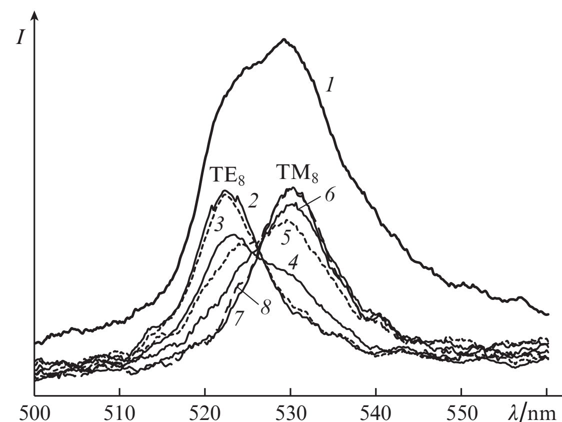


**Figure 6.** Fragments of ASE luminescence spectra in the $Al_{0.5}Ga_{0.5}N$ film without a polariser (*1*) and with it at the turn angles $\zeta$ = (*2*) 0, (*3*) 15, (*4*) 30, (*5*) 45, (*6*) 60, (*7*) 75, and (*8*) 90 ang deg.

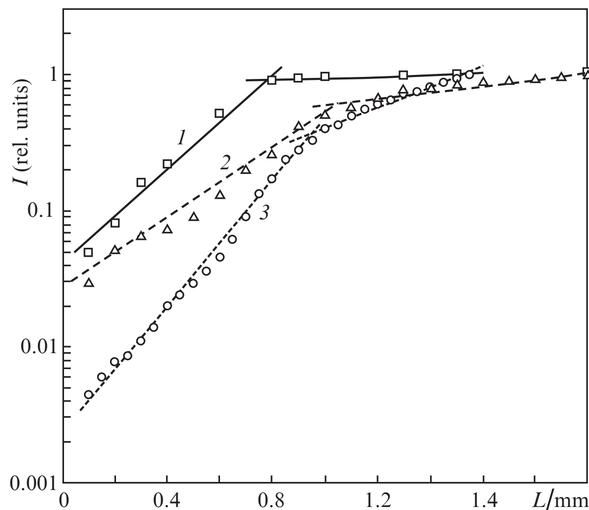


**Figure 7.** ASE luminescence intensity vs. the excitation zone length $L$ for (*1*) $Al_{0.74}Ga_{0.26}N$, $\lambda \approx 468$ nm, (*2*) $Al_{0.5}Ga_{0.5}N$, $\lambda \approx 528$ nm, and (*3*) $AlN/Al_{0.6}Ga_{0.4}N/AlN$, $\lambda \approx 475$ nm; $P_p = 220$ kW cm$^{-2}$.

can see that $I$ exponentially increases with $L$ in the range 0–1 mm. At $L > 0.8$–1 mm, the intensity $I$ in $Al_xGa_{1-x}N$/AlN structures saturates, whereas saturation in $AlN/Al_{0.6}Ga_{0.4}N/AlN/Al_2O_3$ is absent.

An oscillogram of a SE pulse at $\lambda \approx 595$ nm for an $Al_{0.5}Ga_{0.5}N$ film is shown in Fig. 8. One can see that the pulse shape is determined by at least two processes characterised by the times of fast ($\tau_f$) and slow ($\tau_s$) attenuation of the emission intensity. In the same figure, variation of $\tau_f$ is shown as a function of the pump power density $P_p$.

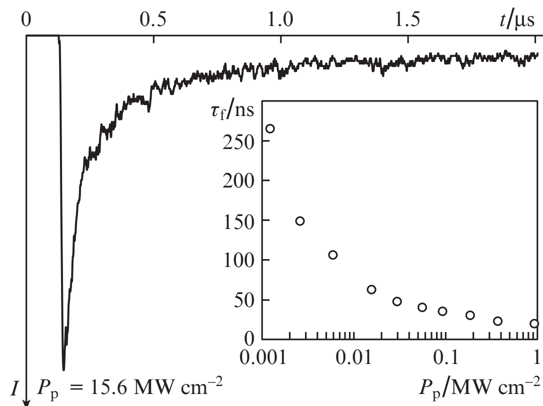


**Figure 8.** Oscillogram of the SE pulse from a cleaved edge in $Al_{0.5}Ga_{0.5}N$, $\lambda = 595$ nm. Dependence of $t_f$ on $P_p$ (in the inset).

The values of the measured quantum yield for spontaneous emission in $Al_{0.74}Ga_{0.26}N$, $Al_{0.65}Ga_{0.35}N$, and $Al_{0.5}Ga_{0.5}N$ films are 0.79, 0.49, and 0.14, respectively.

## 3. Discussion of results

The threshold character of the emission intensity growth with increasing excitation density ($P_p \geqslant 15$ kW cm$^{-2}$) and its exponential growth with the length of the excitation zone in the range $L = 0$–1 mm show the amplifying properties of $Al_xGa_{1-x}N$ films under optical pumping. Since the emission propagates in a waveguide structure, its spectral characteristics should be determined by the waveguide parameters. Consider the $Al_{0.5}Ga_{0.5}N/AlN/Al_2O_3$ structure, which is presented by an asymmetrical waveguide comprised of an AlGaN film with the refractive index $n_1 \approx 2.244$ [26], a buffer AlN layer with $n_2 \approx 2.085$ [27], and a sapphire substrate with $n_3 \approx 1.77$ [27] (the refractive indices are given for the case $\lambda = 530$ nm). External surfaces of the structure have a contact with air possessing $n_0 \approx 1$. In this case, $n_1 > n_2 > n_3 > n_0$ and, consequently, there are several critical incident angles $\Theta_{cr}$ for emission corresponding to the total internal reflection at the media boundaries: $\Theta_{10} = \arcsin(n_0/n_1) \approx 26.5°$ for the $Al_{0.5}Ga_{0.5}N$–air interface, $\Theta_{12} = \arcsin(n_2/n_1) \approx 68°$ for the $Al_{0.5}Ga_{0.5}N$–AlN interface, $\Theta_{23} = \arcsin(n_3/n_2) \approx 58.3°$ for the AlN–$Al_2O_3$ interface, and $\Theta_{30} = \arcsin(n_0/n_3) \approx 34.4°$ for the $Al_2O_3$–air interface. The beams passing from an arbitrary point inside the AlGaN film undergo total internal reflection at incident angles exceeding the critical angles [28, 29]. Calculations based on Fresnel formulae [29] show that the reflection coefficient at the $Al_{0.5}Ga_{0.5}N$–AlN interface is small (~0.05%) due to a small difference between the refractive indices of contacting media. As a result, emission from $Al_{0.5}Ga_{0.5}N$ efficiently penetrates into AlN and the total internal reflection for this emission occurs at incident angles greater than $\Theta_{13} = \arcsin(n_3/n_1) \approx 52.1°$. Thus, for angles $68° > \Theta > 52.1°$, the region comprising the $Al_{0.5}Ga_{0.5}N$ film and buffer AlN film can be considered as a united waveguide.

The emission spectral distribution obtained, which comprises a collection of equidistant peaks is explained as follows. The light field in a waveguide comprises a sum of two plane TE and TM waves with mutually orthogonal polarisations. These waves propagate in a zigzag manner; their incident angles are greater than the angles of the total internal reflection on structure interfaces. The model of self-consistent field distribution requires that the total phase shifts in the waves propagating in the film from bottom to top and back be multiple of 2π [28]:

$$2kn_1h\cos\Theta + \delta_1 + \delta_2 = 2\pi m, \quad (1)$$

where $k = 2\pi/\lambda$ is the wavenumber; $h = h_0 + h_p + X_1(\Theta) + X_2(\Theta)$ is the waveguide thickness; $X_1(\Theta)$ and $X_2(\Theta)$ are the Goos–Hanchen shifts [28]; $\delta_1$ and $\delta_2$ are the phase shifts in the total internal reflection on the waveguide boundaries; and $m$ is the integer that defines the mode order. Here, the waveguide thickness $h$ depends on the propagation angle $\Theta$. The phase shifts $\delta_1$ and $\delta_2$ are determined by the Fresnel formulae [29]. According to (1), waveguide propagation of electromagnetic energy in the form of plane uniform waves inside the layer is only possible for a discrete set of incident angles beyond the critical angle of the total reflection.

The modes of a planar waveguide are solutions of the wave equation and are divided by polarisation to TE and TM modes with distinct $\delta_1$ and $\delta_2$. Spontaneous emission propagates chaotically in all directions. Positions of spectral components can be calculated from (1) based on known parameters of the waveguide. These values can be comparable with the experimental data obtained. Waveguide mode parameters for the $Al_{0.74}Ga_{0.26}N$ structure were found by solving the transcendent equation (1) graphically with the experimental wavelength values of emission peak centres $\lambda_i$ presented in Fig. 2. According to (1), the constructed experimental dependences of $S = 2n_2(\lambda_i)/\lambda_i$ on $m$ should be linear functions with

the constant of propotionality $B = [h(\Theta)\cos(\Theta)]^{-1}$. The phase shifts $\delta_1$ and $\delta_2$ in this case can be neglected due to the small values in the considered wavelength range.

The values for $B_k$ were obtained from linear extrapolation of experimental data according to the least-squares method for all structures and each of the TE and TM modes. The propagation angles $\Theta$ for various modes were found by solving the equations $[h(\Theta)\cos(\Theta)]^{-1} - B_k = 0$ graphically. Finally, the unique solution of this equation was obtained for the angle $\Theta$, which turned out to be only one or two degrees greater than the critical angle of the total internal reflection for the structures investigated ($\Theta_{cr} = 55.5°$ for the $Al_{0.74}Ga_{0.26}N$ structure). For TE and TM modes these angles actually coincide. Similar results have been obtained for other structures as well.

Under uniform pumping along the excitation zone, the maximal gain and superluminescence are achieved in the conditions, where the total gain $G \sim g_0 l$ reaches a maximal value ($g_0$ is the gain per unit length, $l$ is the length of the active region). Since the coefficient $g_0$ is constant versus length, in the case of a zig–zag light propagation in the amplifying medium and the total internal reflection, the value of $G$ depends on angle $\Theta$: $G \sim g_0 L/\sin\Theta$. For the same wavelength at $\Theta < \Theta_{cr}$, the total internal reflection from waveguide walls is absent and emission leaves the waveguide actually without amplification; at $\Theta = \Theta_{cr}$ the gain is maximal, and at $\Theta > \Theta_{cr}$ the gain falls because light propagates at a greater angle and the length of the active region becomes shorter.

Emission is coupled out through a film edge under the condition that the incident angle onto the cleaved surface $\Theta$ is less than $\Theta_{10} = 26.5°$, which is impossible in the ideal case. Hence, the emission propagating in the waveguide in the form of generated modes is closed between the waveguide walls. Experiments show that part of the ASE energy penetrates from the $Al_xGa_{1-x}N$ film into a sapphire substrate and leaves the structure edge at a small angle to the waveguide plane. SE propagates within the same angle simultaneously with ASE and with a comparable intensity. As an example, experiments were carried out with the $Al_{0.65}Ga_{0.35}N/AlN/Al_2O_3$ structure for determining the coefficient $T$ of ASE transmission through the $AlN/Al_2O_3$ boundary. For this purpose, we measured part of the ASE energy that passed from a cleaved edge of the sapphire substrate. Taking into account the quantum yield and part of the ASE energy we found that $T \approx 0.4\%$, which makes it possible to estimate the loss per unit length for the electromagnetic waves propagating along the waveguide. The losses obtained $\sim 2 \times 10^{-2}$ cm$^{-1}$ are small as compared to the losses in the case of optical amplification; hence, one can neglect them considering waveguide processes.

Frustrated total internal reflection in this case is explained by the fact that any physical boundary between two media is never a geometrical plane, but has an intermediate layer of certain thickness. With such a layer, the reflection laws are complicated. The Fresnel formulae well describe experimental results for a monochromatic uniform waves. Actually, real electromagnetic waves are nonstationary and spatially inhomogeneous, which leads to imperfect reflection from the interface and, consequently, to violation of the total reflection near the angle $\Theta_{cr}$ [30, 31].

The experiment has shown that the degree of polarisation of spontaneous emission for an $Al_{0.5}Ga_{0.5}N$ film is negligible. Polarisation measurements for ASE revealed two groups of orthogonally polarised peaks with different spectral positions. These are related to TE and TM waveguide modes with mutually orthogonal polarisations and different phase shifts (see Fig. 6).

The exponential growth of the ASE intensity with increasing excitation volume length demonstrates light amplification in the medium. The small-signal intensity of output emission $I(L)$ is determined by the expression [17]:

$$I(L) = (I_0 S/g_0)[\exp(g_0 L) - 1]. \quad (2)$$

Here, $I_0$ is the spontaneous emission power per unit transverse cross section of the excited volume; $S$ is the cross-section area; $g_0 = (g_1 - a)$ is the experimentally observed gain; $g_1$ is the gain due to induced emission; and $a$ is the coefficient responsible for optical losses due to various mechanisms. At a high quantum efficiency, the radiationless losses are low and, hence, $g_0 \approx g_1$.

The excited volume depth is determined by the absorption depth for pump radiation and the diffuse length of charge carriers. The photon energy of ~4.66 eV corresponding to $\lambda$ = 266 nm is in the range of interband transitions for $Al_{0.5}Ga_{0.5}N$, where the absorption coefficient is$(1.0-1.5) \times 10^5$ cm$^{-1}$. This corresponds to the penetration depth of less than 100 nm [32]. The excited zone also expands due to diffusion of electron–hole pairs. The diffusion length in AlGaN does not exceed 150 nm [33]. Thus, we may assume that the depth of the excitation zone in a transverse direction is less than 250 nm. Taking into account the zigzag light path in the waveguide, the pump radiation penetration depths, and absorption of pump radiation, the real gain $g_0$ per unit length of the active medium may reach ~70 cm$^{-1}$ ($\lambda$ = 510 nm) for the $Al_{0.5}Ga_{0.5}N$ structure, $g_0 \approx 20$ cm$^{-1}$ ($\lambda$ = 468 nm) for the $Al_{0.74}Ga_{0.26}N/AlN$ structure, and $g_0 \approx 44$ cm$^{-1}$ ($\lambda$ = 468 nm) for the $Al_{0.6}Ga_{0.4}N/AlN$ structure.

The decay of the output emission intensity after pulsed excitation in the first approximation is characterised by a sum of two exponents with the times $\tau_f$ and $\tau_s$. A gradual reduction of $\tau_f$ is observed in the whole range of the pump power tested. At a small power $P_p$, the value of $\tau_f$ characterises the time of spontaneous decay for upper levels of the lasing transition. A contribution of radiationless losses in this case can be neglected due to a high quantum efficiency. Issuing from this, the transition cross section $\sigma$ and the concentration of excited centres $N$ can be estimated by the formulae [34]

$$g_0 = N\sigma, \quad \sigma = \sqrt{\frac{\ln 2}{\pi}} \frac{A}{4\pi c n^2} \frac{\lambda^4}{\Delta\lambda}, \quad (3)$$

where $A = 1/\tau$ is the Einstein coefficient. For luminescence of an $Al_{0.5}Ga_{0.5}N$ film possessing $\tau_f \approx 265$ ns (see Fig. 8, $P_p \approx 0$) at $\lambda$ = 590 nm and $\Delta\lambda$ = 180 nm, the cross section is $\sigma \approx 6 \times 10^{-19}$ cm$^2$. Thus, at $g_0 \approx 70$ cm$^{-1}$ the value of population inversion in the excited medium is $N \approx 10^{20}$ cm$^{-3}$, which well correlates with the concentration of doped silica atoms $n_{Si} \approx 3 \times 10^{20}$ cm$^{-3}$ obtained from measurements by the SIMS method.

The wideband photoluminescence is explained by superposed donor–acceptor and zone–acceptor transitions. The donor is silica on the place of the cation $Si_{III}$. Probably, the acceptor is a thrice charged cation vacancy $V_{III}^{-3}$, which is also responsible for the compensation of the $Si_{III}$ donor [35]. The luminescence is determined by the recombination of donor–acceptor pairs, which results in photon emission with the energy dependent on a donor–acceptor distance [13]. If the concentration of emitting defect centres is above ~$10^{15}$ cm$^{-3}$ then these start interacting with each other [36]. Energy

parameters of emission from a separate donor–acceptor pair (DAP) depend on the distance $r$ between the donor and acceptor. The value of $r$ determines the energy of the photon emitted on the DAP transition:

$$E_{h\nu} = E_g - E_d - E_a + e^2/(\varepsilon r), \quad (4)$$

where $E_g$ is the width of the forbidden bandgap; $E_d$ and $E_a$ are the donor and acceptor energies, respectively; $e$ is the electron charge; and $\varepsilon$ is the dielectric constant of the structure. The latter summand in (4) describes the electrostatic interaction between the donor and acceptor. The minimal distance $r$ in the structures studied is the lattice period $d$, and for typical values $d \approx 3.5 \times 10^{-8}$ cm, $\varepsilon \approx 9$ for AlN, GaN, and AlGaN [37], this term can be estimated as 0.5 eV, which by an order of magnitude coincides with the experimental width of spontaneous luminescence spectra. The emission profile of a separate DAP characterised by certain distance $r$ is homogeneous. Since there is a distribution of a large number of DAPs over various $r$, the latter cannot be considered as completely independent oscillators. An ensemble of narrow overlapping lines will produce a continuous inhomogeneously broadened profile. A typical example in Fig. 3 presents approximation of an emission spectrum corresponding to a Gaussian distribution. Similar results were obtained for other samples investigated.

A band structure for AlGaN films and possible scheme of electron–optical transitions are shown in Fig. 9. According to this scheme, the population inversion can be conventionally realised in four stages: 1) energy interaction, which excites transition of electrons from a valence to conduction band; 2) fast trapping of nonequilibrium electrons to donor levels [13]; 3) light emission in donor–acceptor recombination; and 4) fast relaxation of electrons from acceptor states to the valence band. The population inversion can be obtained between the states $N_3$ and $N_4$. Since the electron transitions occur according to the four-level scheme, such an active medium has a low generation threshold.

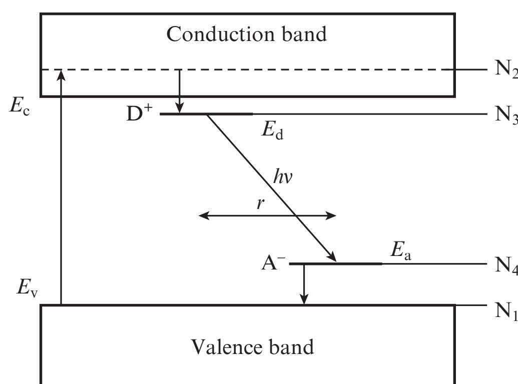


**Figure 9.** Band structure and transitions in AlGaN films.

## 4. Conclusions

Spectral, temporal, and polarisation photoluminescence characteristics have been studied for $Al_xGa_{1-x}N$ structures of various design ($x = 0.5-1$) heavily doped with silica at $n_{Si} > 10^{20}$ cm$^{-3}$ under optical pulsed pumping at $\lambda = 266$ nm. The dominating wideband emission obtained with the bandwidth of ~150 nm covers the whole visible range. Spectra of spontaneous emission are inhomogeneously broadened. The spectrum of emission from a structure edge is split to narrow almost equidistant components determined by the mode structure of the produced plane waveguide. In turn, each component comprises two (TE and TM) modes with mutually orthogonal polarisations. The measured values of the gain $g_0$ are 70 cm$^{-1}$ for $Al_{0.5}Ga_{0.5}N$/AlN at $\lambda = 510$ nm, 20 cm$^{-1}$ for $Al_{0.74}Ga_{0.26}N$/AlN at $\lambda = 468$ nm, and 44 cm$^{-1}$ for AlN/$Al_{0.6}Ga_{0.4}N$/AlN/$Al_2O_3$ at $\lambda = 480$ nm. The values of the quantum efficiency measured for spontaneous emission are 0.79, 0.49, and 0.14 for the $Al_{0.74}Ga_{0.26}N$, $Al_{0.65}Ga_{0.35}N$, and $Al_{0.5}Ga_{0.5}N$ films, respectively. The calculated cross section for the transition related to donor–acceptor transitions is ~$10^{-18}$ cm$^2$. The data obtained confirm promising employment of heavily doped $Al_xGa_{1-x}N$ structures as working materials in lasers tunable in a wide wavelength range.

## References

1. Seong T.-Y., Han J., Amano H., Morkoç H. *III-Nitride Based Light Emitting Diodes and Applications, Topics in Applied Physics* (Dordrecht: Springer, 2013) Vol. 126.
2. Sizov D., Bhat R., Zah Ch.-E. *J. Lightwave Technol.*, **30**, 679 (2012).
3. Razeghi M., Henini M. *Optoelectronic Devices: III–Nitrides* (Amsterdam: Elsevier, 2004).
4. Moustakas Th.D. *MRS Commun.*, **6**, 247 (2016).
5. Nakamura S., Senoh M., Nagahama S., Iwasa N., Matsushita T., Yamada T., Matsushita T., Kiyoku H., Sugimoto Y., Kozaki T., Umemoto H., Sano M., Chocho K. *Appl. Phys. Lett.*, **72**, 2014 (1998).
6. Ivanov S.V., Sorokin S.V., Sedova I.V., in *Molecular Beam Epitaxy: From Research to Mass Production*. Ed. by M. Henini (Amsterdam: Elsevier, 2013).
7. Tischenko V.N., Grachev G.N., Pavlov A.A., Smirnov A.L., Pavlov Al.A., Golubev M.P. *Fiz. Tverd. Tela*, **55**, 2058 (2013).
8. Kneissl M., Kolbe T., Chua C., Kueller V., Lobo N., Stellmach J., Knauer A., Rodriguez H., Einfeldt S., Yang Z., Johnson N.M., Weyers M. *Semicond. Sci. Technol.*, **26**, 014036 (2011).
9. Yoshida H., Kuwabara M., Yamashita Y., Takagi Y., Uchiyama K., Kan H. *New J. Phys.*, **11**, 125013 (2009).
10. Asif Khan M., Shatalov M., Maruska H.P., Wang H.M., Kuokstis E. *Jpn. J. Appl. Phys.*, **44** (P.1), 7191 (2005).
11. Nakamura S., Pearton S., Fasol G. *The Blue Laser Diode* (Berlin: Springer, 2000).
12. Bokhan P.A., Gugin P.P., Zakrevsky Dm.E., Zhuravlev K.S., Malin T.V., Osinnykh I.V., Solomonov V.I., Spirina A.V. *J. Appl. Phys.*, **116**, 113103 (2014).
13. Osinnykh I.V., Malin T.V., Plyusnin V.F., Suranov A.S., Gilinsky A.M., Zhuravlev K.S. *Jpn. J. Appl. Phys.*, **55**, 05FG09 (2016).
14. Zhuravlev K.S., Osinnykh I.V., Protasov D.Yu., Malin T.V., Davydov V.Yu., Smirnov A.N., Kyutt R.N., Spirina A.V., Solomonov V.I. *Phys. Stat. Sol. C*, **10**, 315 (2013).
15. Osinnykh I.V., Malin T.V., Plyusnin V.F., Zhuravlev K.S., Ber B.Ya., Kazantsev D.Yu. *J. Phys.: Conf. Ser.*, **816**, 012002 (2017).
16. Ayupov B.M., Zarubin I.A., Labusov V.A., Sulyaeva V.S., Shayapov V.R. *J. Opt. Technol.*, **78**, 350 (2011).
17. Shaklee K.L., Nahory R.E., Leheny R.F. *J. Lumin.*, **7**, 284 (1973).
18. Oster A., Erbert G., Wenzel H. *Electron. Lett.*, **33**, 864 (1997).
19. KubinR.F., Fletcher A.N. *J. Lumin.*, **27**, 455 (1982).
20. Il'chenko S.N., Kostin Yu.N., Kukushkin I.A., Ladugin M.A., Lapin P.I., Lobintsov A.A., Marmalyuk A.A., Yakubovich S.D. *Quantum Electron.*, **41**, 677 (2011) [*Kvantovaya Elektron.*, **41**, 677 (2011)].
21. Lapin P.I., Mamedov D.S., Marmalyuk A.A., Padalitsa A.A., Yakubovich S.D. *Quantum Electron.*, **36**, 315 (2006) [*Kvantovaya Elektron.*, **36**, 315 (2006)].

22. Mamedov D.S., Prokhorov V.V., Yakubovich S.D. *Quantum Electron.*, **33**, 471 (2003) [*Kvantovaya Elektron.*, **33**, 471 (2003)].
23. Andreeva E.V., Il'chenko S.N., Ladugin M.A., Lobintsov A.A., Marmalyuk A.A., Shramenko M.V., Yakubovich S.D. *Quantum Electron.*, **43**, 994 (2013) [*Kvantovaya Elektron.*, **43**, 994 (2013)].
24. Kryukov P.G. *Quantum Electron.*, **31**, 95 (2001) [*Kvantovaya Elektron.*, **31**, 95 (2001)].
25. Kryukov P.G. *Phys. Usp.*, **183**, 897 (2013) [*Usp. Fiz. Nauk*, **183**, 897 (2013)].
26. Sanford N.A., Robins L.H., Davydov A.V., Shapiro A., Tsvetkov D.V., Dmitriev A.V., Keller S., Mishra U.K., DenBaars S.P. *J. Appl. Phys.*, **94**, 2980 (2003).
27. Antoine-Vincent N., Natali F., Mihailovic M., Byrne D., Semond F., Massies J. *J. Appl. Phys.*, **93**, 5222 (2003).
28. Kogelnik H. *IEEE Trans. Microwave Theory Techniques*, **23**, 2 (1975).
29. Born M., Wolf E. *Principles of Optics* (Cambridge: Cambridge University Press, 1980).
30. Kukharchik P.D., Serdyuk V.M., Titovitskii I.A. *Zh. Tekh. Fiz.*, **69** (4), 74 (1999).
31. Sviridov A.P. *Quantum Electron.*, **37**, 1 (2007) [*Kvantovaya Elektron.*, **37**, 1 (2007)].
32. Muth J.F., Brown J.D., Johnson M.A.L., Yu Z., Kolbas R.M., Cook J.W., Schetzina J.F. *MRS Internet J. Nitride Semicond. Res.*, **4S1**, G5.2 (1999).
33. Malin T.V., Gilinsky A.M., Mansurov V.G., Protasov D.Yu., Kozhuhov A.S., Yakimov E.B., Zhuravlev K.S. *Semiconductors*, **49**, 1285 (2015).
34. Kück S. *Appl. Phys. B*, **72**, 515 (2001).
35. Osinykh I.V., Malin T.V., Zhuravlev K.S., Bokhan P.A., Zakrevskii D.E., Fateev N.V. *Tezisy Dokl. XIII Ross. Konf. 'Fizika Poluprovodnikov'* (Proceedings of the XIII Russian Conference on Semiconductor Physics) (Ekaterinburg, 2017) p. 316.
36. Yu P.Y., Cardona M. *Fundamentals of Semiconductors. Physics and Materials Properties* (New York: Springer, 2002).
37. Quay R. *Gallium Nitride Electronics* (Berlin: Springer-Verlag, 2008).